






Continuous release of $O_2^{\cdot-}/ONOO^-$ in plasma-exposed HEPES-buffered saline promotes TRP channel-mediated uptake of a large cation

Shota Sasaki¹  | Yuexing Zheng¹ | Takayuki Mokudai² |
Hiroyasu Kanetaka^{3,4}  | Masanori Tachikawa^{4,5,6}  | Makoto Kanzaki⁴  |
Toshiro Kaneko¹ 

¹Graduate School of Engineering, Tohoku University, Aoba-ku, Sendai, Japan

²Institute for Materials Research, Tohoku University, Aoba-ku, Sendai, Japan

³Graduate School of Dentistry, Tohoku University, Aoba-ku, Sendai, Japan

⁴Graduate School of Biomedical Engineering, Tohoku University, Aoba-ku, Sendai, Japan

⁵Graduate School of Pharmaceutical Sciences, Tohoku University, Aoba-ku, Sendai, Japan

⁶Graduate School of Biomedical Sciences, Tokushima University, Tokushima, Japan

Correspondence

Shota Sasaki, Graduate School of Engineering, Tohoku University, 6-6-05 Aoba, Aramaki, Aoba-ku, Sendai 980-8579, Japan,
Email: s.sasaki@tohoku.ac.jp

Funding information

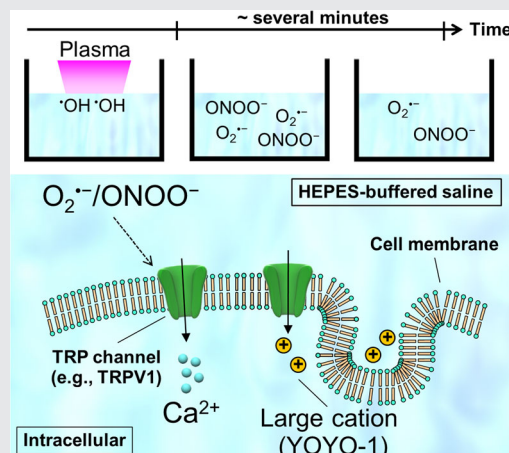
Research Institute of Electrical Communication, Tohoku University; Japan Society for the Promotion of Science, Grant/Award Numbers: 15J01427, 16K12863, 16K13708, 18H03687, 19K14698, 24108004; Frontier Research Institute for Interdisciplinary Sciences, Tohoku University

Abstract

Although the externally controllable extracellular supply of the short-lived reactive oxygen and nitrogen species, such as $O_2^{\cdot-}$, $\cdot NO$, and $ONOO^-$, could potentially manipulate cellular functions, their simple administration to cells is likely to be ineffective due to their rapid deactivation. In this study, we found a method of a continuous supply of $O_2^{\cdot-}/ONOO^-$ over a few minutes, which is triggered by irradiation of a nonequilibrium atmospheric pressure plasma to commonly used organic buffers (e.g., 4-(2-hydroxyethyl)-1-piperazineethanesulfonic acid, HEPES). In addition, a continuous low-dose $O_2^{\cdot-}/ONOO^-$ supply was shown to induce a physiologically relevant Ca^{2+} response and subsequently the uptake of a large cation mediated by transient receptor potential channel family member(s). Our results provide a novel approach to the continuous $O_2^{\cdot-}/ONOO^-$ supply, requiring controllable and mass-volume treatments.

KEYWORDS

atmospheric pressure plasma, Ca^{2+} signaling, peroxynitrite, plasma medicine, TRP channel



This is an open access article under the terms of the Creative Commons Attribution License, which permits use, distribution and reproduction in any medium, provided the original work is properly cited.

© 2020 The Authors. *Plasma Processes and Polymers* published by Wiley-VCH Verlag GmbH & Co. KGaA

1 | INTRODUCTION

Reactive oxygen species (ROS) and reactive nitrogen species (RNS) were initially recognized as toxic, and they have been extensively studied.^[1,2] However, in recent years, it has become apparent that modest levels of ROS and RNS play important signaling roles in many cellular processes such as growth, response to environmental stimuli, and programmed cell death. Among ROS and RNS, nitric oxide ($\cdot\text{NO}$), the superoxide anion radical ($\text{O}_2^{\cdot-}$), and peroxynitrite (ONOO^-) formed from the former two species are known to regulate many processes via their unique chemical properties.^[3-5] If the roles of these reactive species can be fully understood and the supply to cells can be actively controlled, they may offer promising treatments for a variety of conditions. However, these species are highly reactive and are consumed at a high rate under a physiological condition (37°C, pH 7.4) generating other ROS and RNS via complex reaction systems; hence, it is difficult to elucidate their roles and control their supply.

In such situations, an ONOO^- donor, capable of continuously supplying living cells with ONOO^- , was developed and utilized. 3-(4-Morpholinyl)sydnone imine hydrochloride (SIN-1), which spontaneously decomposes in the presence of molecular oxygen to generate $\cdot\text{NO}$ and $\text{O}_2^{\cdot-}$, is a well-known ONOO^- donor.^[6-8] However, the ONOO^- supply occurs by spontaneous autolysis and is not controllable in a time- and site-dependent manner. In addition, SIN-1 itself or SIN-1 derivatives often have undesired effects on cells. As an alternative, the continuous ONOO^- supply was reported using a system combining nitric oxide synthase (NOS) and xanthine oxidase.^[9,10] However, the simultaneous use of different materials, particularly enzymes, makes the reaction system extremely complicated. In addition, some reagents described are expensive and not suitable for large volume treatment.

Recently, medical applications of a nonequilibrium atmospheric pressure plasma (APP) have attracted attention.^[11,12] Plasma, the fourth state of matter, is generally an ionized gas that consists of a significant number of energetic electrons, ions, free radicals, excited species, photons, and so forth. Compared with general thermal plasma, a nonequilibrium APP has a lower gas (ion) temperature, with a quite high-electron temperature (~several eV). This allows for strong nonequilibrium chemical reactions derived from the energetic electrons and highly efficient productions of gaseous reactive species. Thus, a nonequilibrium APP can generate a variety of gaseous ROS and RNS, including $\text{O}_2^{\cdot-}$ and $\cdot\text{NO}$ from oxygen (O_2), nitrogen (N_2), and water (H_2O) in ambient air, and it can directly deliver these to a target without

any thermal damage.^[13,14] This technology can potentially give us a catalyst-free, high-throughput supply of short-lived ROS and RNS to regulate cellular processes. In fact, several innovative medical applications have been reported such as the selective killing of cancer cells and wound healing.^[11,12,15,16] However, as mentioned above, short-lived species such as $\text{O}_2^{\cdot-}$ and $\cdot\text{NO}$ are instantly deactivated under physiological conditions,^[5] and it is difficult to deliver these to tissue regions through a bulk liquid. Therefore, not less short-lived but more long-lived ROS and RNS (e.g., H_2O_2 , NO_2^- , and NO_3^-) are likely to be key factors in many cases.

In the present study, by utilization of nonequilibrium APP irradiation as a reactive trigger and subsequently by the production of $\text{O}_2^{\cdot-}$ with oxidation of 4-(2-hydroxyethyl)-1-piperazineethanesulfonic acid (HEPES; a widely used organic buffer), we established a method of continuous $\text{O}_2^{\cdot-}/\text{ONOO}^-$ supply at a 10^4 -fold lower cost, compared with SIN-1 as a conventional method (based on ONOO^- generation, moles per USD, calculated from prices given by Sigma-Aldrich; Figure S1). In addition, we demonstrated the uptake of a large cation induced by a continuous low-dose $\text{O}_2^{\cdot-}/\text{ONOO}^-$ supply and the potential of APP-exposed HEPES as a drug permeation enhancer. These results may lead to new findings in not only drug delivery but also in a wide range of fields that may benefit from a controllable, continuous $\text{O}_2^{\cdot-}/\text{ONOO}^-$ supply, requiring a mass-volume treatment.

2 | MATERIALS AND METHODS

2.1 | Plasma irradiation system

A nonequilibrium APP was generated, as shown in Figure 1. Helium gas served as the working gas, with its flow rate (f) through the dielectric tube being regulated by a mass flow controller, and typically, $f = 3$ L/min. When a high voltage (V_{p-p}) with a frequency of approximately 9 kHz was applied between the two electrodes, with the powered electrode being a 1.5-mm diameter tungsten rod and the other being a hot plate, an APP was generated, flowing from the nozzle of the quartz glass tube into the ambient air. The distance between the bottom edge of the electrode and the edge of the nozzle was 23 mm. The APP was exposed to HEPES-buffered saline (HBS; containing 150-mM NaCl, 5-mM KCl, 2-mM CaCl_2 , 1-mM MgCl_2 , 5.6-mM D-glucose, and 10-mM HEPES [pH adjusted to 7.4 with NaOH]), with or without various ROS/RNS probes, in a glass-bottomed recording chamber (D11131H; Matsunami, Osaka, Japan) kept on the hot plate (37°C). The APP exposure time was defined as t_i . The discharge power was obtained on the basis of the Q - V Lissajous characteristics. Q was measured using a 22-nF

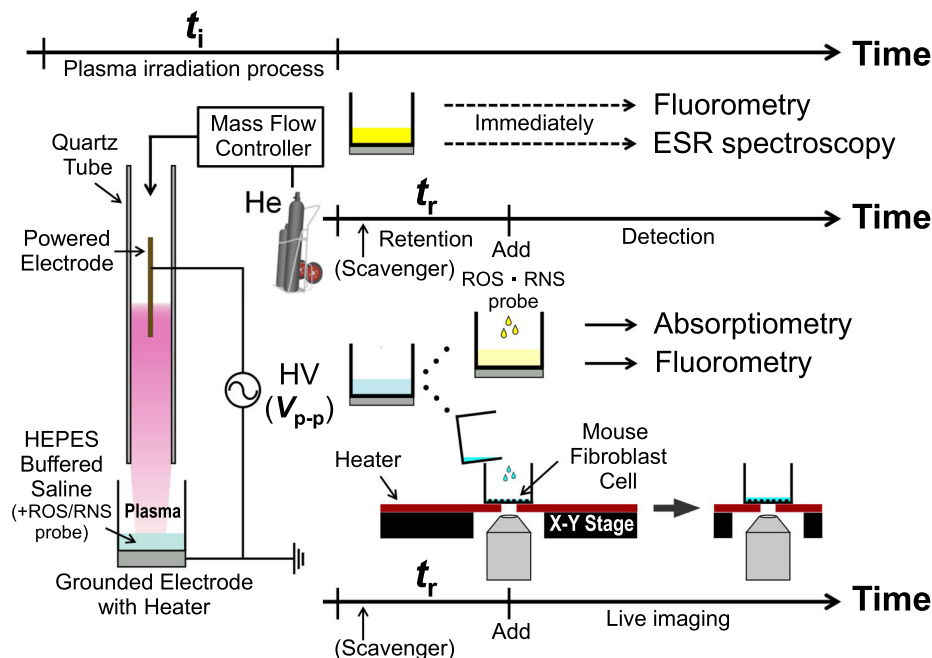


FIGURE 1 The experimental apparatus and procedures of measurements of reactive species generation, $[Ca^{2+}]_i$ response, and YOYO-1 uptake induced by a nonequilibrium atmospheric pressure plasma

capacitor inserted between the lower electrode and the ground. The calculated mean powers were 1 and 2.5 W for $V_{p-p} = 5.0$ and 6.0 kV, respectively.

2.2 | Measurement of $\cdot OH$ generated during APP irradiation

In total, four different chemical probes were used for $\cdot OH$ detection. Each chemical probe was added to HBS before the APP irradiation, and the fluorescence or the electron spin resonance (ESR) spectrum of the solution was obtained immediately after the irradiation process, respectively.

Terephthalate anion, which is produced from terephthalic acid, reacts with $\cdot OH$ to form 2-hydroxyterephthalate ion as a highly fluorescent material with a rate constant of $(4.4 \pm 0.1) \times 10^9 \text{ M}^{-1} \cdot \text{s}^{-1}$.^[17,18] Although the reaction reportedly requires the dissolved oxygen, it would not matter in the present study, because the decrease in the dissolved oxygen concentration by the He blow would not be so fast as shown in Reference [19]. Three milliliters of 2 mM TA/HBS was treated and measured.

2-[6-(4'-Hydroxy)phenoxy-3H-xanthen-3-on-9-yl]benzoic acid (HPF; SK3001-01; Goryo Chemical, Sapporo, Japan) and 2-[6-(4'-amino)phenoxy-3H-xanthen-3-on-9-yl]benzoic acid (APF; SK3001-02; Goryo Chemical) are highly sensitive to $\cdot OH$ among other reactive species (e.g., $O_2^{\cdot -}$, H_2O_2 , 1O_2 , and NO).^[20-22] APF is sensitive to peroxyxynitrite

(ONOO⁻) and also hypochlorite ion (OCl⁻); thus, the difference in selectivity of HPF and APF helps us to speculate the reactive product that is dominantly generated on some assumptions (higher scavenging rates compared with other competitive reactions and negligible decomposition of the probe product). Three milliliters of 10- μM HPF or APF/HBS was treated and measured.

5,5-Dimethyl-1-pyrroline *N*-oxide (DMPO) reacts with $\cdot OH$ at a high rate ($4.3 \times 10^9 \text{ M}^{-1} \cdot \text{s}^{-1}$) and produces paramagnetic DMPO-OH adduct.^[23] One milliliter of 175-mM DMPO/water was treated and measured using an X-band ESR spectrometer (FES-FA100; JEOL, Tokyo, Japan). The measurement conditions were the following: 4-mW microwave power; 9.43-GHz microwave frequency; center field: 336.898-mT; field sweep width; 100-kHz field modulation; 0.1-mT modulation width; 0.03-s time constant; and 60-s sweep time.

2.3 | Measurement of HEPES-derived radical cations, H_2O_2 , NO_2^- , and ONOO⁻ in APP-exposed HBS

The ESR spectrum of HEPES-derived radical cations was obtained using the X-band ESR spectrometer. The ESR measurements of the treated HBS ($t_i = 300 \text{ s}$, VS: 500 μl) were consecutively conducted at room temperature after the APP exposure process. The measurement conditions were the following: 4-mW microwave power; 9.43-GHz

microwave frequency; center field: 337.454 mT; field sweep width; 100-kHz field modulation; 0.2-mT modulation width; 0.03-s time constant; and 60-s sweep time. Then, the aging time was defined as the time between the completion of the APP exposure process and the middle of the sweeping procedure.

Three different chemical probes were used for the detection of H_2O_2 , NO_2^- , and ONOO^- . Each chemical probe was added to 100- μl HBS at a prescribed time (t_r) after the completion of the APP exposure process ($t_i = 2$ s). When a scavenger was used, it was added 10 s after the completion of the APP exposure process. The concentrations of H_2O_2 and NO_2^- were obtained using chemical kits based on Trinder's reagent and Griess reagent (WAK- H_2O_2 and WAK- NO_2 ; Kyoritsu Chemical-Check Laboratory, Tokyo, Japan), respectively. The generation of ONOO^- was evaluated using a 1,3,5,7-Tetramethyl-2,6-dicyano-4,4-difluoro-8-[2-(2-hydroxy-2-oxoethoxy)-4-hydroxyphenyl]-3a,4-dihydro-3a-aza-4a-azonia-4-bora(IV)-s-indacene (NiSPY-3; SK3003-01, Goryo Chemical). The fluorescence of NiSPY-3 is specifically enhanced upon the reaction with ONOO^- , among other reactive species (e.g., $\cdot\text{OH}$, OCl^- , $\text{O}_2^{\cdot-}$, H_2O_2 , $^1\text{O}_2$, and NO).^[24] A solution of 5-mM NiSPY-3/dimethyl sulfoxide (DMSO) was added to the treated HBS (final concentration of NiSPY-3 was 10 μM) and its fluorescence was immediately measured.

2.4 | Cell culture

Mouse 3T3-L1 fibroblasts (American type culture collection [ATCC] CL-173) and human breast adenocarcinoma MCF-7 cells (RBRC-RCB1904) were obtained from ATCC and RIKEN BioResource Center, respectively. 3T3-L1 fibroblasts were maintained in Dulbecco's modified Eagle's medium (DMEM) supplemented with 10% calf serum (CS), 100-U/ml penicillin, and 100- $\mu\text{g}/\text{ml}$ streptomycin (growth medium) at 37°C in an 8% CO_2 atmosphere. For observation, cells were re-plated onto glass-bottomed recording chambers and cultured for 1–3 additional days.

2.5 | Measurement of changes in cytosolic free Ca^{2+} concentration ($[\text{Ca}^{2+}]_i$) and YOYO-1 uptake

The acetoxymethyl (AM) ester form of fluo-4 (F-14201; Invitrogen, Carlsbad, CA) was dissolved in DMSO at 5 mM. 3T3-L1 cells in a glass-bottomed recording chamber were incubated in serum-free DMEM-HG containing 5 μM fluo-4 AM and 0.03% Cremophor EL (C5135, Sigma-Aldrich, St. Louis, MO) for 30 min at 37°C. The cells were then washed with HBS. Images were acquired

every 2 s using a confocal microscope (FV1000; Olympus, Tokyo, Japan). Changes in $[\text{Ca}^{2+}]_i$ ($\Delta F_{[\text{Ca}^{2+}]_i}$) were expressed as $(F - F_0)/F_0$, where F and F_0 represent the fluorescence intensity of fluo-4 and the averaged fluorescence intensity of the dye before stimulation with APP-exposed HBS, respectively. Further details of the measurement can be found in Reference [25].

The membrane-impermeable fluorescent dye YOYO-1 (Y3601; Molecular Probes, Eugene, OR) was dissolved in DMSO at 1 mM. One hundred microliters of 10- μM YOYO-1/HBS was prepared and kept at 37°C. The solution was exposed to the APP ($t_i = 2$ s). After washing the cells with HBS, the treated YOYO-1/HBS was added to the cells at a prescribed time (t_r) after the completion of the APP exposure process. Fluorescence images of the cells (which correlated with intracellular YOYO-1 levels) were acquired every 20 s using fluorescence microscopy (CKX41; Olympus).

The fluorescence images of $[\text{Ca}^{2+}]_i$ and YOYO-1 uptake were analyzed at the single-cell level using ImageJ, and $\Delta F_{[\text{Ca}^{2+}]_i}$ and ΔF_{YOYO} represent the mean value of 50 cells selected randomly.

2.6 | Determination of SIN-1 concentration

3-(4-Morpholinyl)sydnonimine hydrochloride (SIN-1; S264; Dojindo, Kumamoto, Japan) was used to confirm the contribution of ONOO^- to the uptake of the large cation. The concentration of SIN-1 was determined from the measurement result of time-course changes in $\text{H}_2\text{O}_2/\text{NO}_2^-$ concentration. The amount of ONOO^- release was roughly estimated from the increases in $\text{H}_2\text{O}_2/\text{NO}_2^-$ concentration from $t_r = 30$ to 600 s, and in 80 μM , SIN-1/HBS was almost equivalent to that in the APP-exposed HBS ($t_i = 2$ s, VS: 100 μl ; Figure S2).

3 | RESULTS

3.1 | Production of hydroxyl ($\cdot\text{OH}$) radicals in a solution by He-APP irradiation

When a solution is exposed to an APP formed in the ambient air, a wide variety of ROS and RNS, high-energy electrons, metastable molecules, and photons are generated in the gas phase, which can trigger radical chain reactions upon entering the aqueous phase.^[13,14,26–37] The hydroxyl radical, $\cdot\text{OH}$, is a representative of APP-generated ROS transferred to the liquid phase, which reportedly plays an important role in the radical chain

reactions in a solution. Figure 2 shows that $\cdot\text{OH}$ was generated in significant quantities by He-APP irradiation. Terephthalic acid, HPF, and APF, known as $\cdot\text{OH}$ probes, exhibited clear fluorescence after APP irradiation, and the fluorescence spectra agreed with literature and technical reports.^[17,18] Fluorescence intensities increased linearly with APP irradiation time (Figure 2a-c), indicating that $\cdot\text{OH}$ was generated at a constant rate. The increased rates of APF and HPF ($\Delta\text{intensity}/\Delta t_i$) were approximately 0.582 and 0.337, respectively. The fluorescence increase ratio of APF to HPF was approximately 1.72. This ratio is reported to indicate the nature of the production reaction; for example, the values for $\cdot\text{OH}$ production via the Fenton reaction, ONOO^- , and OCI^- were 1.64, 4.67, and 600, respectively.^[20] Thus, it was expected that a relatively large amount of $\cdot\text{OH}$ would be generated. However, $\cdot\text{OH}$ reacts with Cl^- and organic compounds at a high rate and HBS contains a high concentration of NaCl (150 mM), glucose (5.6 mM), and HEPES (10 mM).^[38,39] Furthermore, the distribution density of $\cdot\text{OH}$ generated during the APP irradiation would not be expected to be spatially homogeneous and recombination reactions of $\cdot\text{OH}$ would be faster in the

high-density regions. Therefore, only a portion of the $\cdot\text{OH}$ produced would survive to be scavenged with the chemical probes.

In an attempt to detect most of the APP-generated $\cdot\text{OH}$ under less competitive reactions, water with highly concentrated (175 mM) DMPO, a spin trapping reagent, was used. After APP irradiation, a clear ESR signal of DMPO- OH was observed and linearly increased with the irradiation time, as shown in Figure 2d. In addition, the ESR signal of DMPO-H was also observed, indicating the generation of H^\cdot during irradiation. Thus, it was confirmed that APP irradiation produced significant amounts of $\cdot\text{OH}$ in solution.

3.2 | Continuous release of O_2^- and ONOO^- in plasma-exposed HBS

If a relatively large amount of $\cdot\text{OH}$ is generated during the APP irradiation, it should react with organic compounds in HBS. Here, we focused on the reaction with HEPES because it had been reported that HEPES-derived radical cations are formed electrolytically at a potential of +0.8 V or via a reaction with any strong oxidant such as

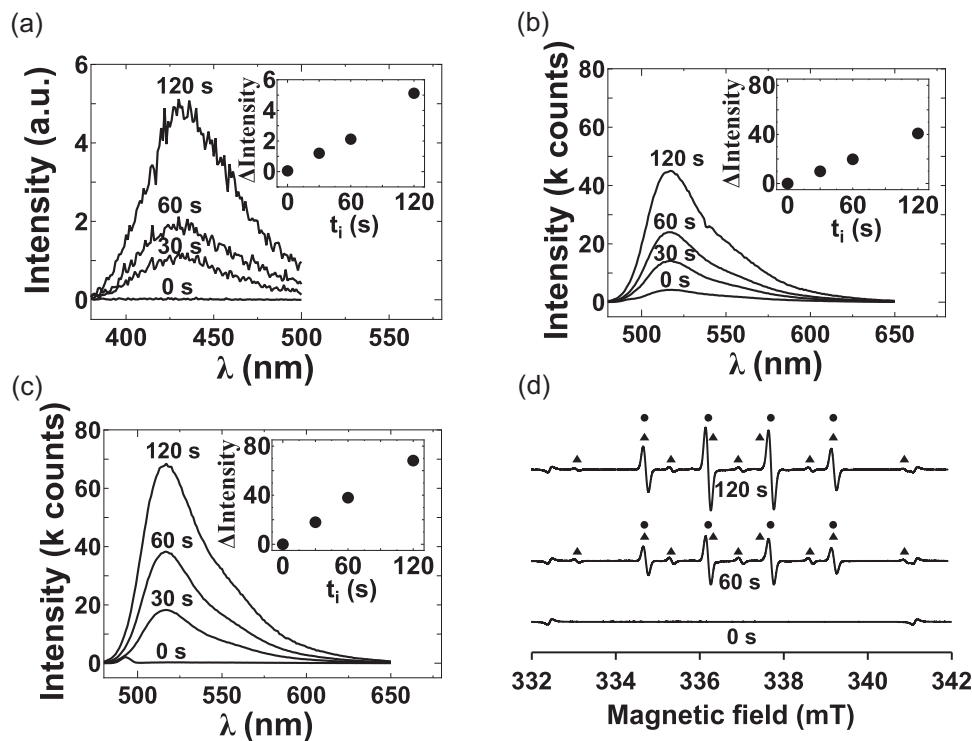
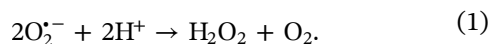


FIGURE 2 $\cdot\text{OH}$ production in significant quantities during APP irradiation. Fluorescence spectra of APP-exposed HBS containing (a) terephthalic acid, (b) HPF, and (c) APF as a function of the APP irradiation time (t_i). (d) ESR spectra of APP-exposed water containing DMPO as a function of t_i . DMPO- OH (black plot, \bullet) and DMPO-H (black plot, \blacktriangle) were shown. (b,c) are reproduced from Reference [21], and further details of the measurement can be found in Reference [21]. APF, 2-[6-(4'-amino)phenoxy-3H-xanthen-3-on-9-yl]benzoic acid; APP, atmospheric pressure plasma; DMPO, 5,5-dimethyl-1-pyrroline *N*-oxide; ESR, electron spin resonance; HBS, HEPES-buffered saline; HEPES, 4-(2-hydroxyethyl)-1-piperazineethanesulfonic acid

$\cdot\text{OH}$ and ONOO^- .^[40,41] The typical ESR spectrum of the APP-exposed HBS, as shown in Figure 3a, is in good agreement with that of HEPES-derived radical cations reported in the literature.^[40] The integrated signals grew over time (Figure 3b), showing that radical generation from HEPES was continuous over a period of several minutes even after the APP irradiation. In addition, LC-MS measurements of the APP-exposed HEPES buffer detected the presence of ions whose molecular weights were the same as the proposed HEPES-derived radical cations (data are not shown). Kirsch et al.^[41] reported that $\text{O}_2^{\cdot-}$ was released during the process of the radical generation in the presence of dissolved oxygen (O_2), and they proposed a detailed reaction sequence. If the proposed scheme was correct, $\text{O}_2^{\cdot-}$ could be potentially released over a period of several minutes in our system. Under the physiological condition in the present study (37°C and pH 7.4), $\text{O}_2^{\cdot-}$ should instantly dismutate to H_2O_2 and O_2 .



The rate constant of the pseudo-second-order reaction was reported to be approximately $2 \times 10^5 \text{ M}^{-1} \cdot \text{s}^{-1}$

at room temperature and pH 7.4.^[42] In fact, the H_2O_2 concentration of the APP-exposed HBS did increase over time (Figure 3c), and the time-course was similar to that of the HEPES-derived radical cations. Furthermore, the addition of superoxide dismutase (SOD) promoted an increase in H_2O_2 concentration (Figure 3d). These results are consistent with the proposed release of $\text{O}_2^{\cdot-}$.

However, not only ROS but also RNS are known to be generated by APP irradiation.^[28,30–32,43,44] If $\cdot\text{NO}$ or a precursor of $\cdot\text{NO}$ was generated in the APP-exposed HBS, it should react with the released $\text{O}_2^{\cdot-}$ to form ONOO^- at a diffusion-controlled rate ($k = 4.3\text{--}6.7 \times 10^9 \text{ M}^{-1} \cdot \text{s}^{-1}$).^[5,10,45,46] The major proposed reaction pathways of $\cdot\text{NO}$ and ONOO^- are as follows^[5,47–50]:

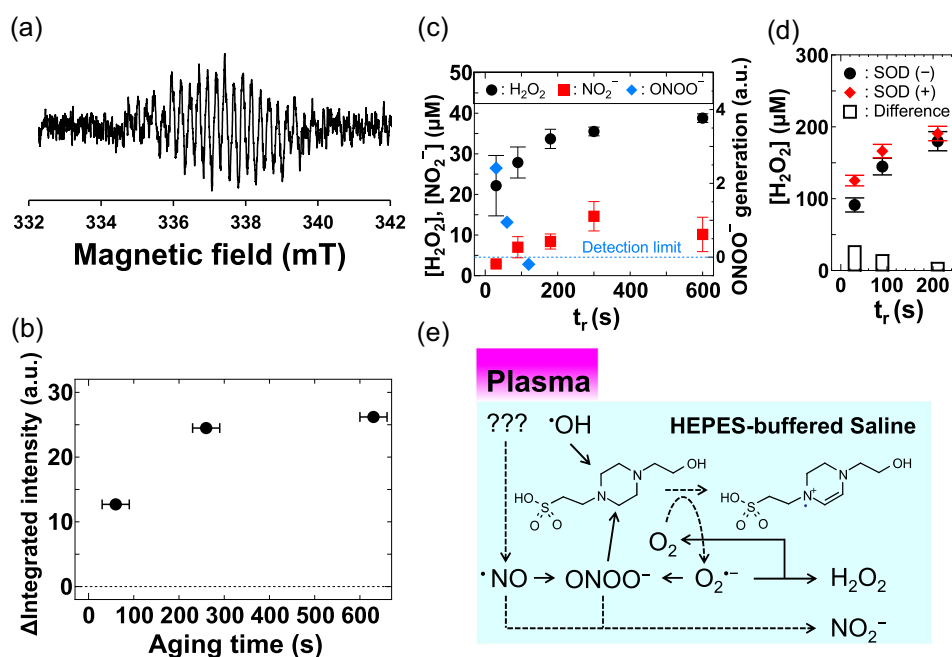
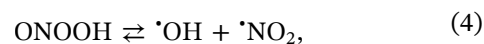
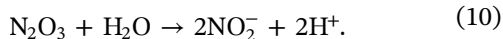
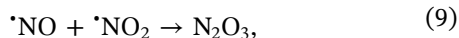
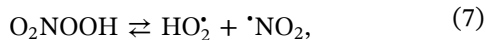


FIGURE 3 A continuous $\text{O}_2^{\cdot-}/\text{ONOO}^-$ release in APP-exposed HBS. (a) Typical ESR spectrum of APP-exposed HBS and (b) the integrated ESR intensity as a function of aging time. (c) Concentrations of H_2O_2 (black plot, \bullet) and NO_2^- (red plot, \blacksquare), and fluorescence intensity of APP-exposed HBS containing NiSPY-3 (ONOO^- generation; blue plot, \blacklozenge) as a function of the retention time (t_r). (d) H_2O_2 concentration in APP-exposed HBS with (red plot, \blacklozenge) or without (black plot, \bullet) SOD as a function of the retention time (t_r). Here, the t_r is the time from the completion of the APP exposure process until the addition of the ROS/RNS probes to the APP-exposed HBS, as shown in Figure 1. (e) The proposed mechanism of continuous $\text{O}_2^{\cdot-}/\text{ONOO}^-$ release in the APP-exposed HBS. APP, atmospheric pressure plasma; ESR, electron spin resonance; HBS, HEPES-buffered saline; HEPES, 4-(2-hydroxyethyl)-1-piperazineethanesulfonic acid; ROS, reactive oxygen species; RNS, reactive nitrogen species; SOD, superoxide dismutase



If these reaction pathways were active, NO_2^- should have been continuously produced as one of the end products. An investigation of NO_2^- concentration, based on Griess' assay, did show the continuous production of NO_2^- (Figure 3c). In addition, ONOO^- generation in the APP-exposed HBS was verified using NiSPY-3 as a selective ONOO^- probe, with the generation rate decreasing over time. These results support the view that at least some of the reactions described above occurred after APP irradiation.

Interpreting the abovementioned results, together with the supporting literature and certain inferences, we propose a partial mechanism for a continuous $\text{O}_2^{\cdot-}/\text{ONOO}^-$ release in the APP-exposed HBS, as shown in Figure 3e. Strong oxidizing species such as $\cdot\text{OH}$ are generated during the APP irradiation, which then triggers HEPES oxidation. $\text{O}_2^{\cdot-}$ is released in the oxidation process, and it can react with $\cdot\text{NO}$ to form ONOO^- . ONOO^- can also oxidize HEPES ($k \sim 184 \text{ M}^{-1} \text{ s}^{-1}$), and $\text{O}_2^{\cdot-}$ can be regenerated.^[41] The cyclic reaction could play a major role in the sustained supply of short-lived reactive species.

3.3 | TRP channel-related YOYO-1 uptake enhanced by a continuous release of $\text{O}_2^{\cdot-}$ and/or ONOO^-

We have previously reported that unidentified products in the APP-exposed HBS can trigger a physiologically relevant TRP channel-mediated Ca^{2+} influx in 3T3L1 fibroblasts.^[25] In this study, we showed that the uptake of a large cation (YOYO-1) with a molecular weight of 1,271 Da is promoted in APP-exposed HBS, and the relationship between the TRP channel and the chemical reactions analyzed above will be further discussed in this study.

As previously reported, the administration of plasma-exposed HBS to cells in culture resulted in gradual and sometimes oscillatory increases in $[\text{Ca}^{2+}]_i$ after a 70-s lag period, as shown in Figures 4a and 4c. On the other hand, the YOYO-1 uptake was significantly enhanced by the administration of APP-exposed HBS containing YOYO-1 after a longer lag period (~ 600 s). Both increased $[\text{Ca}^{2+}]_i$ and YOYO-1 uptake reached maxima and then declined as t_r increased (Figure 4d,e), indicating that the $\text{O}_2^{\cdot-}/\text{ONOO}^-$ release, which becomes deactivated over

time, as shown above, may be responsible for these cellular responses. As shown in Figure 4f,g, both increased $[\text{Ca}^{2+}]_i$ and YOYO-1 uptake were almost completely prevented in the presence of ruthenium red (RR), a noncompetitive, pan inhibitor of multiple TRP channels.^[51–53] Furthermore, we confirmed that human breast cancer cells MCF-7, which exhibited less $[\text{Ca}^{2+}]_i$ sensitivity to APP-exposed HBS, acquired plasma responsiveness after the moderate exogenous expression of TRPV1 channels (Figure S3). Thus, the APP-induced $[\text{Ca}^{2+}]_i$ and YOYO-1 uptake increases may result from signal transductions mediated by TRP channel family member(s).

To make sure that the $\text{O}_2^{\cdot-}$ and/or ONOO^- release in the APP-exposed HBS was involved in the enhancement of YOYO-1 uptake, the effect of the addition of SOD to the APP-exposed HBS and HBS with SIN-1 (an ONOO^- donor) was investigated (Figure 4h). The addition of SOD catalyzed the dismutation of $\text{O}_2^{\cdot-}$, as shown in Figure 3d, and significantly suppressed the APP-enhanced uptake but did not completely inhibit it. This observation was also consistent with the incomplete suppression of the increase in H_2O_2 concentration ($\text{O}_2^{\cdot-}$ release). In addition, the effect of HBS with SIN-1 on YOYO-1 uptake was almost equivalent to that with APP. Thus, it was concluded that $\text{O}_2^{\cdot-}/\text{ONOO}^-$ was likely to be a major factor determining APP-induced YOYO-1 uptake.

4 | DISCUSSION

$\cdot\text{NO}$, $\text{O}_2^{\cdot-}$, and ONOO^- play important roles in many physiological processes, and many of these have been extensively investigated. In particular, a low-dose supply of these reactive species has been implicated in the regulation of critical cellular functions; also, they have been considered as potent mediators of cellular damage due to their strong oxidizing nature. Key findings of the present study are that APP exposure of HBS initiates a unique chain reaction, resulting in a low-level release of $\text{O}_2^{\cdot-}/\text{ONOO}^-$ that induced TRP-mediated uptake of YOYO-1. However, much about the mechanism remains unclear, and there are many open questions regarding the reaction mechanism.

One question inquired the cause for the longer lifetimes of HEPES-derived radical cations in this study than those reported by Kirsch et al.^[41] They found that the corresponding ESR signals decayed with half-lives of about 10–15 min at 20°C, whereas the half-lives in our case were more than 60 min. Therefore, the decay processes, here, might differ from the previous reaction systems. In addition, although previous reports showed H_2O_2 formation ($\text{O}_2^{\cdot-}$ release) from PIPES as well as

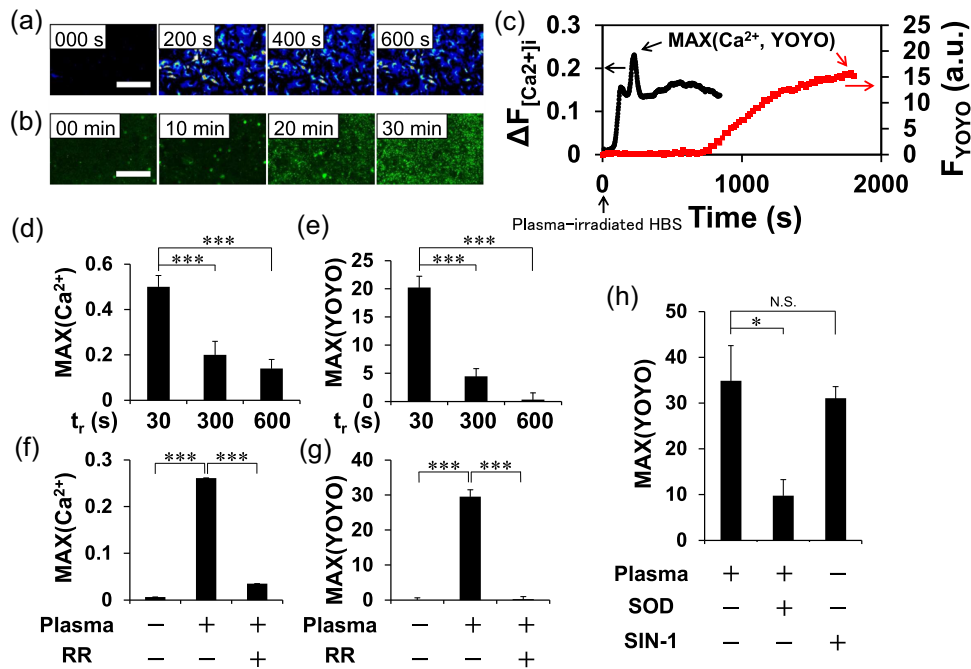


FIGURE 4 Time-lapse images showing changes in (a) $[Ca^{2+}]_i$ and (b) YOYO-1 uptake in 3T3-L1 cells stimulated with plasma-exposed HBS, and (c) the average $[Ca^{2+}]_i$ ($\Delta F_{[Ca^{2+}]_i}$) and YOYO-1 uptake (F_{YOYO-1}) as a function of time. Scale bars represent (a) 1 mm and (b) 200 μ m. Max values of (d,f) $\Delta F_{[Ca^{2+}]_i}$ and (e,g) F_{YOYO-1} as a function of (d,e) t_r and (f, g) RR dependence. Here, retention time (t_r) is the time from completion of the APP exposure process until the addition of the APP-exposed HBS, as shown in Figure 1. (h) The effect of SOD and SIN-1 on max values of F_{YOYO-1} . The mean values \pm standard error obtained from 23 cells ($[Ca^{2+}]_i$) and 50 cells (YOYO-1) are shown. The statistical analysis was performed with the Mann–Whitney U test and Steel–Dwass test for multiple comparisons ($*p < .05$, and $***p < .001$). At least three independent experiments were performed; representative results are shown. (a), (d), and (f) are reproduced from Reference [25] and further details of the measurement can be found in Reference [25]. APP, atmospheric pressure plasma; HBS, HEPES-buffered saline; HEPES, 4-(2-hydroxyethyl)-1-piperazineethanesulfonic acid; RR, ruthenium red; SIN-1, 3-(4-Morpholinyl)sydnone imine hydrochloride; SOD, superoxide dismutase

HEPES, clear differences among four Good's buffers were confirmed (Figure S4). In our system, H_2O_2 was continuously formed from HEPES and HEPPSO but not from PIPES or POPSO, which suggested the involvement of HEPES other than $O_2^{\cdot-}$ release with oxidation. It has also been reported that HEPES may be oxidized by hypochlorite (OCl^-),^[54] which could be generated via the reaction of APP-generated $\cdot OH$ or $\cdot O$ with Cl^- . However, the generation of OCl^- was estimated to be lower than that of $\cdot OH$ from the result using HPF and APF. Such alternative reactions may explain the observed differences.

The most important question is as follows: From where does $\cdot NO$, which is assumed to exist after the APP irradiation, originate? If $ONOO^-$ was continuously generated in the APP-exposed HBS, not only $O_2^{\cdot-}$ but also $\cdot NO$ should be released because the half-life of $\cdot NO$ depends on the concentration, and it is also relatively short in the order of μM . However, there is little evidence as to the identity of the $\cdot NO$ precursor. In addition, the difficulty of measurement of $\cdot NO$ in the liquid phase makes it much more difficult to detect and elucidate the chain

reaction involved. The mechanism of $\cdot NO$ -related reactions in our system needs to be further investigated.

In addition, the experiment where the HBS was exposed to the He plasma blow in the open air produced extremely complicated chemistry, and our proposed mechanism, as shown in Figure 3e, would be incomplete. For example, bicarbonate/carbon dioxide (HCO_3^-/CO_2) is known to react with radicals and modulate the reactions mediated by $ONOO^-$. The HCO_3^-/CO_2 may affect the continuous $O_2^{\cdot-}/ONOO^-$ release in the APP-exposed HBS; however, the rate of the reaction of $ONOO^-$ with HCO_3^-/CO_2 ($\sim 3 \times 10^4 M^{-1} \cdot s^{-1}$) seems to be lower than that of the reaction with HEPES.^[55,56]

Our study showed that $[Ca^{2+}]_i$ increase and YOYO-1 uptake was enhanced, probably by the continuous release of $O_2^{\cdot-}/ONOO^-$, and these cellular responses were mediated by one or more TRP channels. In fact, exogenous expression of TRPV1 channels significantly enhanced the sensitivity to APP-exposed HBS (Figure S3). It has also been reported that the $ONOO^-$ -induced $[Ca^{2+}]_i$ increase was significantly suppressed in TRPV1-null mice and inhibited in the presence of FeTPPS, a selective

inhibitor of ONOO⁻.^[57] Therefore, TRPV1 channel could, potentially, be a target of ONOO⁻. TRPV1 activation is considered to trigger the subsequent YOYO-1 uptake, but the mechanism of transmembrane transport remains unclear. One possibility is that YOYO-1 passes directly through the TRP channel pore. A similar large cation, YOPRO-1, was reportedly transferred through the TRPV1 pore.^[58–60] The observed increase in the YOYO-1 uptake in the present study could have a similar mechanism. Considered from a number of different points of view, including the above, research indicates that TRP channels are promising drug targets.^[61] In addition, [Ca²⁺]_i increase is reported to regulate endocytosis; therefore, some transmembrane transport systems could be activated by a continuous O₂^{•-}/ONOO⁻ supply.

The method reported here, a continuous O₂^{•-}/ONOO⁻ supply triggered by APP irradiation to HBS, might be suitable not only for drug delivery but also for other medical, agricultural, and environmental applications requiring controllable and mass-volume treatments. Although our knowledge is far from complete and the elucidation of the reaction mechanism is challenging, we anticipate that our results will contribute to further progress in scientific fields related to ROS and RNS, leading to valuable, technological applications.

ACKNOWLEDGMENT

This study was supported by JSPS KAKENHI Grant Nos. 24108004, 15J01427, 16K13708, 16K12863, 18H03687, and 19K14698. This study was also supported by the Research Institute of Electrical Communication, Tohoku University, and by Frontier Research Institute for Interdisciplinary Sciences, Tohoku University.

ORCID

Shota Sasaki  <http://orcid.org/0000-0002-1478-7700>

Hiroyasu Kanetaka  <http://orcid.org/0000-0001-7744-3879>

Masanori Tachikawa  <http://orcid.org/0000-0001-5711-5691>

Makoto Kanzaki  <http://orcid.org/0000-0002-6884-2955>

Toshiro Kaneko  <http://orcid.org/0000-0003-0552-6151>

REFERENCES

- [1] S. Magder, *Crit. Care* **2006**, *10*, 208.
- [2] R. L. Auten, J. M. Davis, *Pediatr. Res.* **2009**, *66*, 121.
- [3] J. S. Beckman, W. H. Koppenol, *Am. J. Physiol. Physiol.* **1996**, *271*, C1424.
- [4] G. L. Squadrito, W. A. Pryor, *Free Radicals Biol. Med.* **1998**, *25*, 392.
- [5] P. Pacher, J. S. Beckman, L. Liaudet, *Physiol. Rev.* **2007**, *87*, 315.
- [6] N. Hogg, V. M. Darley-Usmar, M. T. Wilson, S. Moncada, *Biochem. J.* **1992**, *281*, 419.
- [7] R. J. Singh, N. Hogg, J. Joseph, E. Konorev, B. Kalyanaraman, *Arch. Biochem. Biophys.* **1999**, *361*, 331.
- [8] J. L. Trackey, T. F. Uliasz, S. J. Hewett, *J. Neurochem.* **2001**, *79*, 445.
- [9] H. Rubbo, R. Radi, M. Trujillo, R. Telleri, B. Kalyanaraman, S. Barnes, M. Kirk, B. A. Freeman, *J. Biol. Chem.* **1994**, *269*, 26066.
- [10] R. Radi, G. Peluffo, M. N. Alvarez, M. Naviliat, A. Cayota, *Free Radicals Biol. Med.* **2001**, *30*, 463.
- [11] G. Fridman, G. Friedman, A. Gutsol, A. B. Shekhter, V. N. Vasilets, A. Fridman, *Plasma. Process. Polym.* **2008**, *5*, 503.
- [12] M. G. Kong, G. Kroesen, G. Morfill, T. Nosenko, T. Shimizu, J. van Dijk, J. L. Zimmermann, *New J. Phys.* **2009**, *11*, 115012.
- [13] P. J. Bruggeman, M. J. Kushner, B. R. Locke, J. G. E. Gardeniers, W. G. Graham, D. B. Graves, R. Hofman-Caris, D. Maric, J. P. Reid, E. Ceriani, *Plasma Sources Sci. Technol.* **2016**, *25*, 53002.
- [14] P. Bruggeman, C. Leys, *J. Phys. D: Appl. Phys.* **2009**, *42*, 53001.
- [15] H. Tanaka, M. Hori, *J. Clin. Biochem. Nutr.* **2017**, *60*, 29.
- [16] M. Keidar, *Plasma Sources Sci. Technol.* **2015**, *24*, 033001.
- [17] R. W. Matthews, *Radiat. Res.* **1980**, *83*, 27.
- [18] S. E. Page, W. A. Arnold, K. McNeill, *J. Environ. Monit.* **2010**, *12*, 1658.
- [19] J.-S. Oh, E. J. Szili, N. Gaur, S.-H. Hong, H. Furuta, H. Kurita, A. Mizuno, A. Hatta, R. D. Short, *J. Phys. D: Appl. Phys.* **2016**, *49*, 304005.
- [20] K. Setsukinai, Y. Urano, K. Kakinuma, H. J. Majima, T. Nagano, *J. Biol. Chem.* **2003**, *278*, 3170.
- [21] S. Sasaki, Y. Hokari, A. Kumada, M. Kanzaki, T. Kaneko, *Plasma. Process. Polym.* **2018**, *15*, e1700077.
- [22] R. Honda, S. Sasaki, K. Takashima, T. Sato, T. Kaneko, *Jpn. J. Appl. Phys.* **2019**, *58*, 106002.
- [23] G. V. Buxton, C. L. Greenstock, W. P. Helman, A. B. Ross, *J. Phys. Chem. Ref. Data* **1988**, *17*, 513.
- [24] T. Ueno, Y. Urano, H. Kojima, T. Nagano, *J. Am. Chem. Soc.* **2006**, *128*, 10640.
- [25] S. Sasaki, M. Kanzaki, T. Kaneko, *Sci. Rep.* **2016**, *6*, 25728.
- [26] T. Verreycken, R. M. van der Horst, N. Sadeghi, P. J. Bruggeman, *J. Phys. D: Appl. Phys.* **2013**, *46*, 464004.
- [27] Q. Xiong, Z. Yang, P. J. Bruggeman, *J. Phys. D: Appl. Phys.* **2015**, *48*, 424008.
- [28] A. F. H. van Gessel, B. Hrycak, M. Jasiński, J. Mizeraczyk, J. van der Mullen, P. J. Bruggeman, *J. Phys. D: Appl. Phys.* **2013**, *46*, 095201.
- [29] S. Yonemori, R. Ono, *J. Phys. D: Appl. Phys.* **2014**, *47*, 125401.
- [30] A. Komuro, R. Ono, T. Oda, *J. Phys. D: Appl. Phys.* **2012**, *45*, 265201.
- [31] T. Murakami, K. Niemi, T. Gans, D. O'Connell, W. G. Graham, *Plasma Sources Sci. Technol.* **2014**, *23*, 025005.
- [32] S. A. Norberg, E. Johnsen, M. J. Kushner, *Plasma Sources Sci. Technol.* **2015**, *24*, 035026.
- [33] A. Tani, Y. Ono, S. Fukui, S. Ikawa, K. Kitano, *Appl. Phys. Lett.* **2012**, *100*, 254103.
- [34] H. Tresp, M. U. Hammer, J. Winter, K. D. Weltmann, S. Reuter, *J. Phys. D: Appl. Phys.* **2013**, *46*, 435401.
- [35] H. Jablonowski, R. Bussiahn, M. U. Hammer, K.-D. Weltmann, T. von Woedtke, S. Reuter, *Phys. Plasmas* **2015**, *22*, 122008.

- [36] Y. Gorbanev, D. O'Connell, V. Chechik, *Chem. - Eur. J* **2016**, 22, 3496.
- [37] C. Chen, D. Liu, A. Yang, H.-L. Chen, M. G. Kong, *Plasma Chem. Plasma Process.* **2018**, 38, 89.
- [38] A. E. Grigor'ev, I. E. Makarov, A. K. Pikaev, *Khimiya Vysok. Ehnergij* **1987**, 21, 123.
- [39] J. K. Thomas, *Trans. Faraday Soc.* **1965**, 61, 702.
- [40] J. K. Grady, N. D. Chasteen, D. C. Harris, *Anal. Biochem.* **1988**, 173, 111.
- [41] M. Kirsch, E. E. Lomonosova, H.-G. Korth, R. Sustmann, H. de Groot, *J. Biol. Chem.* **1998**, 273, 12716.
- [42] B. H. J. Bielski, D. E. Cabelli, R. L. Arudi, A. B. Ross, *J. Phys. Chem. Ref. Data* **1985**, 14, 1041.
- [43] S. Ikawa, A. Tani, Y. Nakashima, K. Kitano, *J. Phys. D: Appl. Phys.* **2016**, 49, 425401.
- [44] Y. Gorbanev, N. Stehling, D. O'Connell, V. Chechik, *Plasma Sources Sci. Technol.* **2016**, 25, 55017.
- [45] J. S. Beckman, T. W. Beckman, J. Chen, P. A. Marshall, B. A. Freeman, *Proc. Natl. Acad. Sci.* **1990**, 87, 1620.
- [46] R. E. Huie, S. Padmaja, *Free Radicals Res. Commun.* **1993**, 18, 195.
- [47] S. Pfeiffer, A. C. F. Gorren, K. Schmidt, E. R. Werner, B. Hansert, D. S. Bohle, B. Mayer, *J. Biol. Chem.* **1997**, 272, 3465.
- [48] S. Goldstein, G. Czapski, J. Lind, G. Merényi, *Chem. Res. Toxicol.* **1999**, 12, 132.
- [49] C. Molina, R. Kissner, W. H. Koppenol, *Dalt. Trans* **2013**, 42, 9898.
- [50] S. Goldstein, G. Czapski, *Inorg. Chem.* **1997**, 36, 4156.
- [51] D. E. Clapham, *Nature* **2003**, 426, 517.
- [52] J. Vriens, G. Appendino, B. Nilius, *Mol. Pharmacol.* **2009**, 75, 1262.
- [53] M. Bencze, M. Behuliak, A. Vavřínová, J. Zicha, *Eur. J. Pharmacol.* **2015**, 765, 533.
- [54] P. Xing, K. Gao, B. Wang, J. Gao, H. Yan, J. Wen, W. Li, Y. Xu, H. Li, J. Chen, *Chem. Commun.* **2016**, 52, 5064.
- [55] O. Augusto, M. G. Bonini, A. M. Amanso, E. Linares, C. C. X. Santos, S. L. De Menezes, *Free Radicals Biol. Med.* **2002**, 32, 841.
- [56] S. Carballal, M. Trujillo, E. Cuevasanta, S. Bartesaghi, M. N. Möller, L. K. Folkes, M. A. García-Bereguiaín, C. Gutiérrez-Merino, P. Wardman, A. Denicola, *Free Radicals Biol. Med.* **2011**, 50, 196.
- [57] N. Ito, U. T. Ruegg, A. Kudo, Y. Miyagoe-Suzuki, S. Takeda, *Nat. Med.* **2013**, 19, 101.
- [58] M.-K. Chung, A. D. Güler, M. J. Caterina, *Nat. Neurosci.* **2008**, 11, 555.
- [59] J. Chen, D. Kim, B. R. Bianchi, E. J. Cavanaugh, C. R. Faltynek, P. R. Kym, R. M. Reilly, *Mol. Pain* **2009**, 5, 3.
- [60] C. H. Munns, M.-K. Chung, Y. E. Sanchez, L. M. Amzel, M. J. Caterina, *J. Biol. Chem.* **2015**, 290, 5707.
- [61] Y. Kaneko, A. Szallasi, *Br. J. Pharmacol.* **2014**, 171, 2474.

SUPPORTING INFORMATION

Additional supporting information may be found online in the Supporting Information section.

How to cite this article: Sasaki S, Zheng Y, Mokudai T, et al. Continuous release of O₂⁻/ONOO⁻ in plasma-exposed HEPES-buffered saline promotes TRP channel-mediated uptake of a large cation. *Plasma Process Polym.* 2020;17:e1900257. <https://doi.org/10.1002/ppap.201900257>